Journal of Membrane Science and Research 6 (2020) 359-366

Journal of Membrane Science & Research

journal homepage: www.msrjournal.com

Research Paper

Physical Studies of Forward Osmosis Membranes Prepared by Cross-linking Polyvinyl Alcohol on Electrospun Nanofibers

Nurafidah Arsat, Juhana Jaafar *, Woei Jye Lau, Mohd Hafiz Dzarfan Othman, Mukhlis A. Rahman, Farhana Aziz, Norhaniza Yusof, Wan Norharyati Wan Salleh, Ahmad Fauzi Ismail

Advanced Membrane Technology Research Centre (AMTEC), School of Chemical and Energy Engineering, Faculty of Engineering, Universiti Teknologi Malaysia, 81310 UTM Johor Bahru, Johor, Malaysia

Article info

Received 2019-12-02
Revised 2020-03-18
Accepted 2020-04-29
Available online 2020-04-29

Keywords

Electrospinning
Electrospun nanofibrous membranes
Composite membranes
Forward osmosis
Polyvinyl alcohol

Highlights

- New dual-layered TFNC-FO membranes
- The best deposition and cross-linking time of PVA
- Physical characterizations showing the presence of PVA top coating
- FO performance comparison with conventional dual-layered composite membranes
- PVA/PVDF composite membranes exhibited a comparable water flux and low J_s/J_w ratio

Graphical abstract

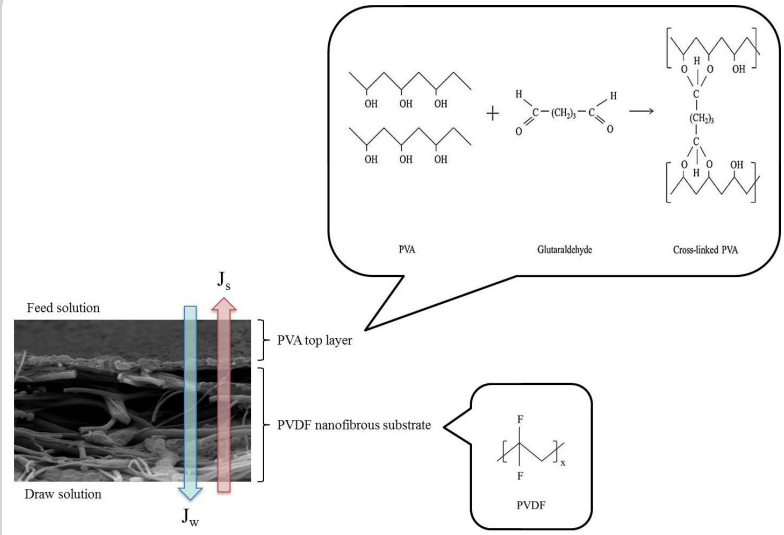

Abstract

The conventional nanofiber-supported forward osmosis (FO) membrane possessed some issues, for example, easy deformation and weak interfacial strength between the substrate and selective layer. A dual-layered composite membrane consists of electrospun nanofibrous membranes (ENMs) as the support layer and cross-linked polyvinyl alcohol (PVA) top coating as the active layer is fabricated. Hence, the objective of this work is to study the physical properties of the prepared PVA/ polyvinylidene fluoride (PVDF) composite membranes. The novelty of this work relies on the new exploitation of the prepared dual-layered thin film nanofibrous composite (TFNC) membranes via the cross-linked technique in the FO process. The experiment works include the fabrication of nanofibrous substrates and selective layer via electrospinning, followed by the PVA cross-linking process prior to the characterisation studies and FO evaluation. FO performance test revealed a comparable water flux with the conventional dual-layered composite membrane, besides exhibited a significantly low J_s/J_w ratio. This study indicated that dual-layered cross-linked PVA on electrospun PVDF nanofibers is a promising approach to overcome the drawback of the existing issues in the conventional method of preparing surface coated composite membranes which is a viable option to manufacture high-performance TFNC-FO membranes.

1. Introduction

Rapid population growth and ongoing economic evolution have led to a substantial rise in demand and access to clean water [1,2]. Among the many strategies adopted to provide affordable and safe drinking water, membrane-based water treatment technologies have drawn intensive interests from academia and industries owing to its merits in generating high-quality water and, in most instances, with lower energy [2]. Forward osmosis (FO), of which is an excellent option to solve the global issue of water shortage, has been commonly used in latest years for water purification as well as seawater desalination owing to the benefits of high rejection efficiencies as well as self-supplied driving forces from osmotic pressure between draw solution and feed solution [3]. In contrast to the existing pressure-driven processes, the FO process in the absence of external hydraulic pressure has important qualities which include a broad range of feed solutions, effective water recovery, high rejection for small compounds, low operating cost, and energy-saving [4,5].

Undoubtedly, both high in rejection and flux are the crucial aims in fabricating filtration membranes. As to improve the water filtration competency, the composite filtration membranes with multilayer composite structures have gained significant attention in water treatment due to their

* Corresponding author: juhana@petroleum.utm.my (J. Jaafar)

DOI: 10.22079/JMSR.2020.117738.1310

precedence of high rejection and good permeability, in addition to their pressure resistance [6,7]. The composite membranes typically consist of a porous substrate with low resistance, which contributes mechanical support for the membrane throughout the process of fabrication, handling and operation, and a thin coating layer on top which acts as a filter [2,6,7]. Both the substrate and the top layer can be customised independently to achieve the optimal and maximise the advantageous characteristics for targeted applications.

Electrospun nanofibrous membranes (ENMs) fabricated through a process known as electrospinning are suitable to be used as the porous substrate for composite membranes, owing to their distinctive properties of interconnected pore structures, exceptional permeability, high surface-to-volume ratio, good mechanical properties, and good water permeability which significantly contribute to water treatment [7-10]. However, due to its high porosity and interconnected structure, a desirable top coating layer is difficult to obtain in the typical fabrication of surface coated composite membranes, as a result of easy penetration of the cast solution into the matrix. Wang et al. [6] reported that dual layer nanofibrous mats consist of a thin top coating made up from polyvinyl alcohol (PVA) nanofiber layer and a porous support layer made up from thick polyacrylonitrile (PAN) nanofiber layer, developed by a facile method that has overcome the disadvantage of easy penetration of the cast solution into the porous support layer in the conventional fabrication of surface covered composite membranes. The crucial technology of their technique included electrospinning of PVA nanofibrous layer on electrospun polymer nanofibrous support, followed by remelting the PVA nanofibrous layer by means of water vapour exposure prior to chemical cross-linking to form a barrier PVA film, in which the composite membranes were later tested for filtration performance using oil and water emulsion separation [6].

In the previous studies, this alternative of developing PVA top coating on nanofibrous support layer as composite membranes showed excellent performance in the separation of oil/water emulsion as well as BSA filtration, as shown in the summarisation of various approaches in Table 1. However, the utilisation of such composite membranes has never been tested as a FO membrane in water purification and desalination application. Hence, as inspired from the facile route introduced by Wang et al. [6], a thin film of PVA which acts as the selective layer has been fabricated on the polyvinylidene fluoride (PVDF) nanofibrous substrate, resulting in thin-film nanofibrous composite (TFNC) membranes was used as FO membrane in this study.

In the current study, PVA nanofibrous layer was fabricated by electrospinning 8% w/v of PVA solution. PVA polymer was chosen because it is biologically compatible and highly hydrophilic, apart from its chemical and thermal stability [11,12]. In addition to its good film-forming properties, highly soluble in water and environmentally friendly, PVA is a polyhydroxy (i.e. –OH groups which are good sites for further reactions) [13]. As to provide PVA the stability in aqueous phase, its water solubility can be reduced by cross-linking this polymer with another material, for instance, the use of glutaraldehyde (GA) in this work. Besides reducing PVA water solubility, the cross-link between PVA and GA will enhance the mechanical strength of the membrane substrate [13]. According to Ray et al. [14], it is hard to dissolve PVA polymer when it is greater than 8% w/v as the molecular weight of PVA is high. Commonly for the case of a highly viscous solution, the polymeric solution may fail to form fibers which can be attributed to electrical charges generating insufficient strength for the stretching purpose [14].

On the other hand, PVDF was chosen as a membrane material for the substrate due to its high mechanical strength, thermal stability, and excellent chemical resistance [15,16], making it suitable for wastewater treatment. Additionally, the reason for choosing PVDF as the material for the support layer is since using hydrophobic membrane substrates for TFNC membranes can minimise the drawbacks of membrane weakening as it is being exposed to liquids due to membrane swelling. Huang et al. [17] demonstrated that a hydrophobic fiber could be used with a surface modified to be hydrophilic to address the swelling issue. In their study, Nylon 6,6 was used to coat PVDF nanofibers to make their surface hydrophilic and this modification exhibited swelling resistance in water.

Using the cross-linked PVA on electrospun PVDF nanofibers, the present work aims to study the physical characteristics of the prepared PVA/PVDF composite membranes. The effect of fabricating PVA thin layer on PVDF nanofibers was accessed using several characterisation methods and followed by the evaluation of FO performance. The implications of cross-linked PVA on ENMs porous substrate were discussed to indicate that dual-layered cross-linked PVA on electrospun PVDF nanofibers is a useful approach to overcome the drawback of the existing issues in the conventional method of preparing surface coated composite membranes. Therefore, it is a viable alternative to manufacture high performance TFNC-FO membranes.

Table 1
Summarization of various approaches to fabricate PVA coating on nanofibrous substrate.

TFNC membranes	Application	Water permeability ($L/m^2.h.bar$)	Rejection (%)	References
PVA/PAN[a]	Oil/water emulsion separation	70 [d]	99.5 [e]	[6]
PVA/PAN[b]	Oil/water emulsion separation	173.90 [e]	99.6 [e]	[18]
PVA/PAN[c]	BSA filtration	57.67 [d]	98.4 [d]	[7]
	Vitamin B_{12} filtration	3.55 [e]	91.1 [e]	[7]

[a] PVA top coating were fabricated using electrospinning technique, remelting through water vapour exposure and crosslinking
[b] PVA top coating were fabricated using electrospraying technique, solution treatment method and crosslinking
[c] PVA top coating were fabricated using electrospraying technique, hot pressing treatment and crosslinking
[d] Was measured using dead-end filtration system
[e] Was measured using cross-flow filtration system

2. Experimental

2.1. Materials

Polyvinylidene fluoride in pellet form (PVDF, Kynar® 760, MW = 440,000 g/mol) and N-methyl-2-pyrrolidone (NMP, >99.5%) provided by Merck were used as the electrospinning polymer and solvent, respectively, for the fabrication of membrane substrate. Polyvinyl alcohol (PVA) with hydrolysis degree of 99% (MW = 89,000 to 98,000 g/mol), and acetone (analytical reagent, 99%) purchased from Merck, glutaraldehyde (GA, 25 wt% solution in water) from Fisher Scientific, as well as hydrochloric acid (HCl, 37%) supplied by RCI Labscan, were utilized in the preparation of PVA barrier layer. Sodium chloride (NaCl, >99.5%) obtained from RCI Labscan was used in the preparation of salt solution for the FO performance test. The deionised (DI) water was produced with a Milli-Q system. All of the chemicals were used without further purification.

2.2. Methods

2.2.1. Electrospinning of PVDF and PVA nanofibers

The fabrication of PVDF nanofibers via electrospinning was started by dissolving PVDF in NMP followed by stirring at 60°C for 12 h to obtain an 18 wt% homogenous solution. A 5 ml volume of precursor solution was loaded into a 10 ml plastic syringe and was carefully ensured that there was no air bubble trapped in the plastic syringe. The syringe diameter was 14.5 mm. The blunt tip metallic needle was connected to the plastic syringe and placed on the syringe pump. The flow rate of the solution was fixed at 1.0 ml/h and controlled by the syringe pump. A voltage of 10.0 kV was applied between the spinneret tip and the collector (rotating metal drum). During the electrospinning process, nanofibers were produced and collected on silicon paper posted on the rotating collector, which rotates at the speed of approximately 200 rpm. The spinneret and the grounded drum were kept at a distance of 15 cm.

Subsequently, the electrospinning of PVA nanofibers on the prepared PVDF nanofibrous mats was started by dissolving PVA in water and stirred at 90°C for 5 h to get 8% w/v homogenous solution. A 2 ml volume of the precursor solution was loaded into the 10 ml plastic syringe and carefully ensured that there was no air bubble trapped in the plastic syringe. The syringe diameter was 14.5 mm. The blunt tip metallic needle was connected to the plastic syringe and placed on the syringe pump. The applied electric voltage was 20.0 kV and the solution feed rate was 1.0 ml/h. The distance between the grounded drum which was covered with PVDF nanofibrous mat beforehand and the spinneret was 18 cm, whereas the rotating collector rotated at the speed of approximately 200 rpm.

2.2.2. Preparation of PVA coating on nanofibrous substrate

In order to produce the PVA/PVDF dual-layer nanofibrous mat, the PVA nanofibers was electrospun on top of the prepared PVDF nanofibrous substrate. The PVA depositing time was varied at 1 and 2 h, separately, to

obtain the best depositing time. The remelting process of the PVA nanofibrous layer was started by treating the prepared dual-layered nanofibrous mats for 10 min using water vapour produced from 90°C water bath, where the distance of the mats from the water bath surface was kept at 10 cm. Since water is an excellent solvent for PVA, when the PVA nanofibrous layer came in contact with water vapour from the water bath, a thin film layer was formed on top of the PVDF nanofibrous substrate as a result from the remelted PVA nanofibers. The PVA/PVDF composite membrane was then cross-linked by soaking the samples in 1:1 volume ratio of DI water/acetone solution which contained 50 mM GA and 20 mM HCl, at room temperature, for 1 and 2 h respectively, to obtain the best crosslinking time. To further enhance the cross-linking process, the composite membranes were placed in 100°C oven for 10 min. Thereafter, the cross-linked composite membranes were kept in DI water prior to use.

2.2.3. Characterizations of substrate membrane and PVA/PVDF composite membranes

The morphology of the pristine PVDF ENMs and composite membranes samples were examined by scanning electron microscopy (SEM) (Hitachi TM3000). The average diameter of electrospun fibers was measured from the SEM image using image analysis software. Prior to the analysis, each surface of the membranes was carefully mounted on the stainless-steel stub using carbon tape. The samples used for cross-sectional analysis were prepared by fracturing the water-wetted membranes in liquid Nitrogen. All of the samples were sputter coated with platinum prior to SEM observation.

The elemental analysis of the substrate membrane and composite membranes samples were studied using energy-dispersive X-ray (EDX) spectroscopy (Hitachi TM3000). Prior to the analysis, each surface of the membranes was carefully mounted on the stainless-steel stub using carbon tape. All of the samples were sputter coated with platinum prior to the EDX observation.

The surface roughness of the pristine PVDF ENMs and composite membranes samples were examined using atomic force microscopy (AFM) (Hitachi AFM5000II) with tapping mode. Prior to AFM analysis, a small piece of each membrane was cut and glued on top of the sample holder. The scanning area was 5 µm x 5 µm to ensure representative surface roughness. The surface roughness parameters were evaluated and expressed in terms of three components; the mean roughness (Ra), Rq/RMS which represents the root mean square of the Z data, and Rz/Rmax which indicates the mean difference between the highest peaks and lowest valleys.

The surface functional groups of the substrate membrane and composite membranes samples were confirmed using Fourier transform infrared (FTIR) spectroscopy (Nicolet iS10, Thermo Scientific) which was equipped with a single reflection attenuated total reflection (ATR) plate. The spectra were measured in transmittance mode from wave number ranging from 4000 to 450 cm^{-1} with 25 scans.

The porosity of the pristine PVDF ENMs and composite membranes samples were measured by mercury intrusion porosimetry (MIP) (AutoPore V 9600, Micromeritics). Mercury was transferred into the chamber where the membrane was placed and the pressure was raised from zero to about 35,000 psia. At each applied pressure, the volume of mercury penetrated into the pores of the membrane was evaluated. Initially, the mercury entered the largest membrane pores at minimum pressure applied. Increasing the pressure forced the mercury to occupy the smaller membrane pores until every pore was filled.

The contact angle (CA) measurements of the substrate membrane and composite membranes samples were determined via sessile drop procedure using a contact angle goniometer (OCA 15Pro, Dataphysics). DI water was used as the liquid with a droplet volume of 1 µL. In order to obtain the contact angle measurements, imaging software was utilised by capturing pictures of water droplets on the membrane surface using a special camera. The measurements were taken at 10 random spots and the average values were calculated for both samples.

2.2.4. Evaluation of FO performance

The FO performance of the prepared composite membranes was tested via a lab-scale cross-flow FO system with 0.0042 m^2 total effective membrane area. The feed and draw solutions which were deionized water and 0.5 mol NaCl solution, respectively, both at ambient temperature were circulated by utilising two variable pumps both fixed at 500 rpm from beginning to end of the process. The process was carried out in the AL-FS operation mode which means that the active layer of the membrane was placed facing the feed solution while the support layer was facing draw solution. The conductivity of the feed solution was measured by a bench conductivity meter (4520, Jenway) and was later converted into concentration using a calibration curve to evaluate the reverse salt flux. The weight changes of draw solution were measured via an electronic balance placed below the draw solution tank to calculate the water flux. The permeate flux, J_w (L m^{-2} h^{-1}, LMH) and reverse solute flux, J_s (g m^{-2} h^{-1}, gMH) can be calculated using Eqs. (1) and (2) as follows:

$$J_w = \frac{\Delta V}{A_m \Delta t} \quad (1)$$

$$J_s = \frac{C_t V_t - C_0 V_0}{A_m \Delta t} \quad (2)$$

where A_m (m^2) is the membrane effective area, ΔV (L) indicate the permeated water volume and Δt (s) indicate the time interval. C_0 (g L^{-1}) and V_0 (L) represent the initial solute concentration and volume of the feed solution, whereas C_t (g L^{-1}) and V_t (L) represent the final solute concentration and volume of the feed solution, respectively.

3. Results and discussion

3.1. Effect of deposition time and cross-linking time of PVA coating on electrospun PVDF substrate

As soon as electrospun PVA nanofibers came in contact with water, they can be dissolved instantly, even though PVA in powder form acts oppositely when coming in contact with water at an ambient temperature. According to Wang et al. [6], PVA nanofibers would absorb water shortly after PVA nanofibrous layer was exposed to water vapour, which later formed a PVA film layer through the remelting process. If the exposure time of PVA nanofibrous layer to water vapour was too short, the resultant film layer would be imperfect with the presence of flaws or small holes on its surface which was caused by insufficient time for the remelting process to occur. In contrast, if the exposure time is too long, PVA nanofibers would be completely dissolved and turned into solution, thus, penetrating the nanofibrous substrate. In respect to this issue, Wang et al. [6] concluded that 10 min would be the appropriate exposure time for the remelting process of PVA nanofibrous layer to occur. Within that particular time, the water condensed on the PVA nanofibrous layer was adequate to remelt and spread in order to produce a film layer that is high in viscosity to prevent the penetration into the substrate layer.

To obtain a PVA thin layer which is insoluble in water, the PVA/PVDF composite membranes which were treated with water vapour were chemically cross-linked by immersing the membrane in DI water/acetone solution that contained GA as the cross-linking agent and HCl as the catalyst. By referring to Park et al. [13], cross-linking bathes consisting of 1:1 volume ratio of DI water/acetone solution which included 50 mM GA and 20 mM HCl were used throughout the current study. Figure 1a,b show the surface SEM images of PVDF nanofibrous substrate covered by cross-linked PVA barrier layer at 1 h of depositing time and 1 h of cross-linking time. It was obviously shown that the surface of the PVDF substrate was not fully coated by PVA thin layer. The PVA nanofibrous layer produced during electrospinning was insufficient to coat the entire surface of the PVDF substrate as a result of short depositing time which led to the inadequate area exposed to water vapour during the remelting process. Hence, to clarify this situation, the duration of depositing time was prolonged.

Concerning the previous issue, with the extended duration of depositing time to 2 h while maintaining the cross-linking time at 1 h, the surfaces became integrated and nonporous, as shown in Figure 1c,d. As compared with the 1 h depositing time, PVA nanofibrous layer spread almost perfectly to form a film layer on the substrate. However, another situation appeared as 1 h of cross-linking time was found to be insufficient for the polymer to react with the cross-linking agent GA in the presence of HCl as the catalyst. Thus, the cross-linking time was prolonged to 2 h while maintaining the depositing time at 2 h. From Figure 1e,f, it can be observed that the PVA top layer covered almost the whole surface of the substrate. Additionally, a three-dimensional network structure seen at the top layer of the composite membranes which was believed to be the main reason for the formation of pores resulted from the intermolecular cross-linking of PVA chains through GA as the cross-linker. Therefore, in this study, the best depositing time for the fabrication of TFNC membranes was 2 h and the best cross-linking time was also 2 h in 1:1 volume ratio of cross-linking bathes (containing GA and HCl in DI water/acetone solution). Table 2 shows the membrane designation based on the preparation variables.

Table 2
Membrane designation based on the preparation variables.

Membrane designation	Preparation variables	
	Depositing time (h)	Cross-linking time (h)
PVA/PVDF1	1	1
PVA/PVDF2	2	1
PVA/PVDF3	2	2

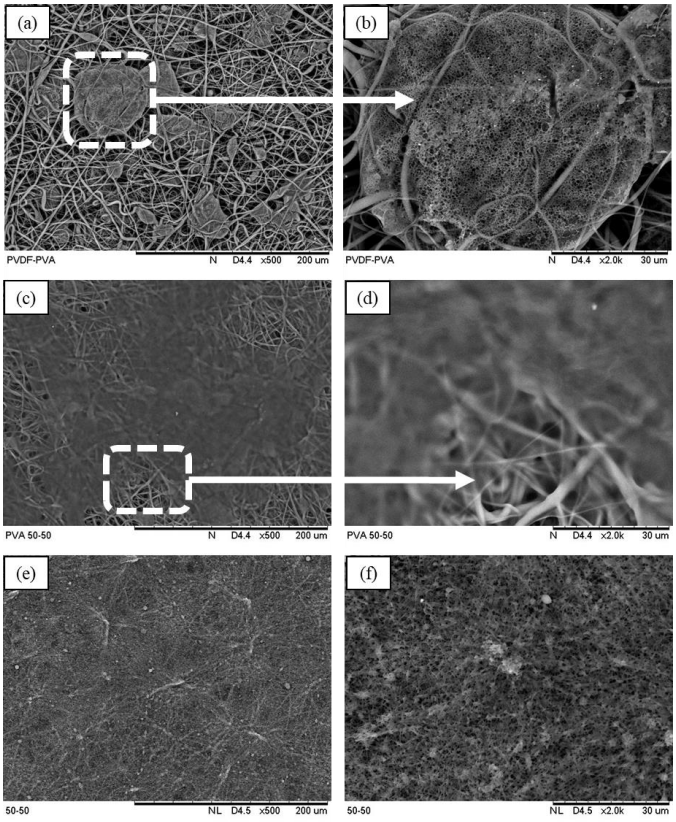

Fig. 1. Top surface SEM images of (a) PVA/PVDF1; (b) higher magnification of PVA/PVDF1; (c) PVA/PVDF2; (d) higher magnification of PVA/PVDF2; (e) PVA/PVDF3; (f) higher magnification of PVA/PVDF3

3.2. Characterizations of substrate membrane and PVA/PVDF3 composite membranes

The prepared pristine PVDF ENMs and composite membranes were characterised by means of SEM, contact angle, EDX, MIP, FTIR, and AFM. The fibrous support of the TFNC membranes was produced by electrospinning process using pristine PVDF. Figure 2a,b show the typical SEM images of PVDF ENMs. As shown in the images, a smooth and bead-free nanofiber mat was obtained in which the diameters of the fibers were mainly distributed in the range of 250 nm to 450 nm. Figure 2c,d demonstrated the chosen PVA/PVDF3 composite membranes with depositing time and cross-linking time both at 2 h, as discussed earlier in Section 3.1. Linked and porous top layer could be observed, and an obvious thin layer above the nanofibrous substrate could also be seen, though the surface was not very flat. This was further verified through EDX analysis shown in Figure 3b which obviously shows the increased peaks of carbon and oxygen as compared with the EDX result for neat PVDF ENMs shown in Figure 3a. The inset of Figure 3 indicates the elements of the membranes in terms of quantitative analysis.

For comparison purposes, the surface contact angle measurement of the substrate and PVA/PVDF3 composite membranes were examined, as shown in the inset of Figure 2a,c, respectively. The obvious difference between the water droplets clearly highlighted that the presence of PVA coating on the PVDF substrate increased the hydrophilicity of the membranes, which was further demonstrated by the apparent decline in contact angle measurement from 130.50° to 48.87°, as presented in Table 3. The high contact angle measurement for pure PVDF ENMs was consistent with other studies on PVDF nanofibers [13,19,20], caused by the properties of PVDF polymer which are hydrophobic in nature and has low surface energy [21]. Meanwhile, the low contact angle measurement of the composite membranes was attributed to the hydrophilic nature of PVA polymer. The hydroxyl (–OH) groups which present abundantly in PVA caused the surface of the composite membranes to be hydrophilic, which led to a water-soluble characteristic. For that reason, in order to form a PVA coating that is highly stable in water, GA which acts as a cross-linker was used by means of acid-catalysed acetalisation, as already proven by Nisola et al. [22]. Based on their study, it is important to note that the crosslinking reaction between GA and PVA involves the formation of the acetal group which was associated with the utilisation of terminal aldehyde groups presence in GA and hydroxyl groups in PVA [22,23]. Therefore, the reduction in hydrophilicity of PVA due to the loss of OH groups caused the coating to be insoluble and stable in water [22].

As for FTIR analysis in Figure 4, a full spectrum of uncoated PVDF ENMs displayed a typical peak structure for PVDF polymer. A strong peak of approximately 1404 cm^{-1} represented C–H stretching vibration while the three peaks at 1274 cm^{-1}, 1171 cm^{-1} and 1071 cm^{-1} corresponded to the presence of C–F bonds which were found in PVDF. A weak wide band between 3200 and 3400 cm^{-1} was associated with O-H stretching due to the strong inter and intra molecular hydrogen bonding in PVA. In addition, the peak of approximately 2949 cm^{-1} was assigned to C–H stretching vibration found in PVA. Another peak at 1698 cm^{-1} was ascribed to C=O groups which confirmed the existence of unreacted remaining aldehyde groups originally from GA after the acetalisation cross-linking process was completed. Therefore, the difference between these two spectra proved the successful coating on PVDF substrate and cross-linking reaction between PVA and cross-linker GA through HCl-catalysed.

As demonstrated by Ahmad et al. [24], the cross-linking duration for the interaction between water vapour treated PVA/PVDF composite membranes with the cross-linker was highly responsible for the distribution of pore size. Prolonged the duration for the cross-linking process to happen might result in further interaction between the hydroxyl groups of PVA and the aldehyde groups presence in GA. However, it is crucial to point out that the crosslinking time which is too long, might cause the membranes to have less hydrophilicity behaviour. In this work, 2h was selected as the best cross-linking time for the interaction between the cross-linker GA and PVA polymer through acid-catalysed using HCl, to occur, without sacrificing the hydrophilicity feature of the resultant membrane.

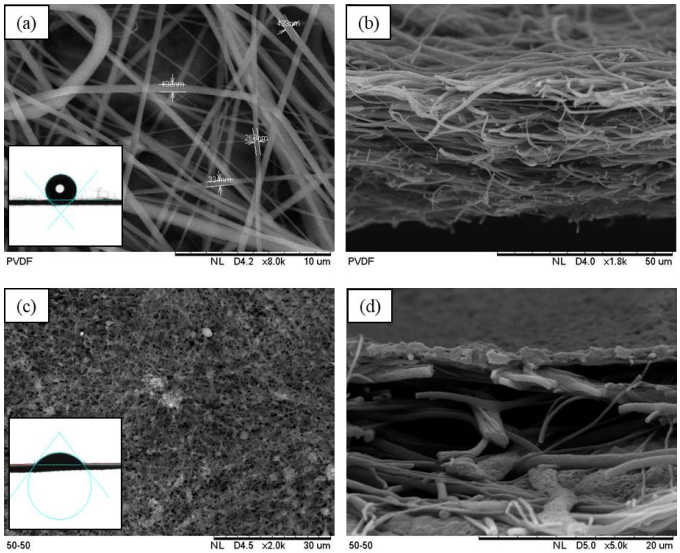

Fig. 2. SEM images of uncoated PVDF and PVA/PVDF3 composite membranes for top surface (a and c) and cross section (b and d).

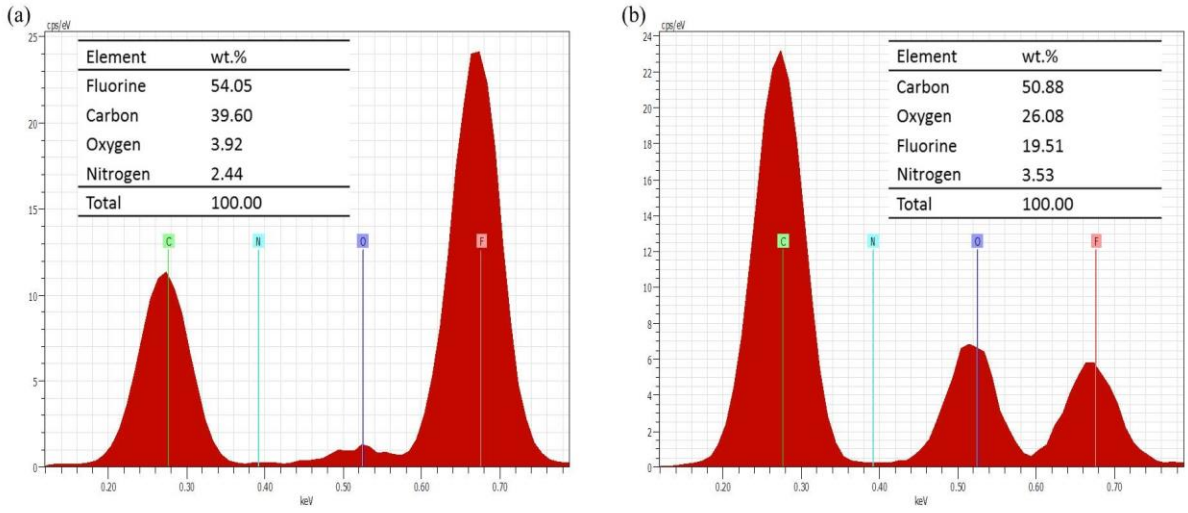

Fig. 3. EDX analysis of (a) pristine PVDF and (b) PVA/PVDF3 composite membranes.

Table 3
Contact angle of pristine PVDF and composite membranes

Membrane	Contact angle (°)
PVDF	130.50 ± 1.43
PVA/PVDF3	48.87 ± 2.30

The physical aspects of the fabricated membranes were further examined in terms of porosity as shown in Table 4. The percentage of porosity shows the percentage of the bulk sample volume that is void space (inter-particle and intra-particle space). The porosity of pristine PVDF was 36.5% and as PVA thin layer was introduced, the percentage of porosity increased to 64.1%. The pore analysis of the fabricated membranes was determined by the mercury intrusion porosimetry. The volume of mercury intruded against the pore diameter of the fabricated membranes was displayed in Figure 5. The curves revealed that the mercury was able to penetrate more through the PVA/PVDF3 composite membranes pores compared to the pristine PVDF. From the curves, the highest volume of mercury intruded was approximately 1.7 mL/g through PVA/PVDF3 composite membranes pores, whereas the highest intrusion through the pristine PVDF pores was approximately 1.1 mL/g.

Table 4
Porosity of pristine PVDF and composite membranes.

Membrane	Porosity, ε (%)
PVDF	36.5
PVA/PVDF3	64.1

Figure 6 shows the pore size distribution of the prepared membranes illustrated as log differential intrusion volume against pore size diameter. The plot shows that the pristine PVDF encompasses multimodal pore size distribution, where the most visible peak can be seen occurring in the range of 100,000 to 200,000 nm. After PVA thin layer was fabricated on PVDF nanofiber support, a strong dissimilarity was observed, which indicated the existence of PVA thin layer, leading to broad distributions shifted to both smaller and bigger diameter of pore size. This is proven as the pore size diameter was moderately distributed in the range of 100,000 and 150,000 nm, and a sharp peak with a narrow distribution appeared in the range of pore size less than 10,000 nm corresponded to the pores which were almost of the same size, whereas a distinctly broad distribution occurred in the range between 250,000 and 350,000 nm. These effects were probably due to the intermolecular cross-linking between the cross-linker GA and PVA chains which resulted in a random three-dimensional network structure, thus, be accountable for the formation of the irregular size of pores.

The AFM images in Figure 7 compared the PVDF nanofiber support and PVA/PVDF3 composite membranes. The AFM image of pristine PVDF nanofibers showed a high nodule-valley like structure which represented the randomly overlapped fiber structure. This structure observed in pure PVDF nanofiber mat was converted into a considerably smoother surface of PVA coated fibers. The random three-dimensional network structure with large pores that indicated the intermolecular cross-linking between the cross-linker GA and PVA chains confirmed the filling of the interstitial voids between the PVDF fibers, as also supported by SEM results in Figure 2. The surface roughness of pristine PVDF and PVA/PVDF3 composite membranes was evaluated and expressed in terms of mean roughness (Ra), Rq/RMS which represented the root mean square of the Z data, and Rz/Rmax which indicated the mean difference between highest peaks and lowest valleys, as presented in Table 5. As observed from the table, there was a reduction in the Ra values from 89.55 nm to 67.21 nm as the PVDF nanofiber support was coated with PVA thin layer. Huang et al. [25] concluded that there are possibilities for the valleys of membranes to be clogged as a result of the absorbed pollutants. Hence, it was advantageous to have membranes with lower roughness since higher membrane roughness contributes to low antifouling abilities. Also, from the surface roughness data, the pristine PVDF shows the high Rz/Rmax value of 519.0 nm, which was reasonable considering the random orientation of nanofibers and the resultant nodule-valley like structure. The Rz/Rmax value of PVA/PVDF3 composite membranes was decreased to 263.5 nm which proved the existence of PVA thin layer on PVDF nanofiber support.

3.3. FO performance of TFNC membranes

Figure 8 presents the FO performance of the prepared dual-layered cross-linked PVA on electrospun PVDF nanofibers (designated as PVA/PVDF3 composite membranes in this study), tested by cross-flow FO system for 1 h operated in AL-FS mode. A dual-layered thin film composite (TFC)-PVDF membrane from previous work by Park *et al.* [13] which consists of polyamide (PA) selective layer on electrospun PVDF nanofibers was used as comparison. The PVA/PVDF3 composite membrane after 20 min of FO process had a slightly higher water flux value of 5.3 LMH compared to 5.1 LMH obtained from the control TFC-PVDF membrane as shown in Figure 8a. However, water flux of PVA/PVDF3 composite membranes decreased slightly with time. This situation is inevitable due to the continuous dilution of draw solution as well as internal concentration polarization (ICP) in the time of FO process. The J_s/J_w values of PVA/PVDF3 composite membranes for 1 h of FO process were ranging from 0.02-0.03 g/L which was significantly low compared with the J_s/J_w value of control TFC-PVDF membrane which was 0.6 g/L as shown in Figure 8b. In this sense, the low value of J_s/J_w ratio indicates the improvement in terms of membrane selectivity besides the reduction in operational cost for draw solution replenishment. These results suggest that the resultant dual-layered cross-linked PVA on electrospun PVDF nanofibers fabricated in this study shows significant potential for practical applications in FO technologies.

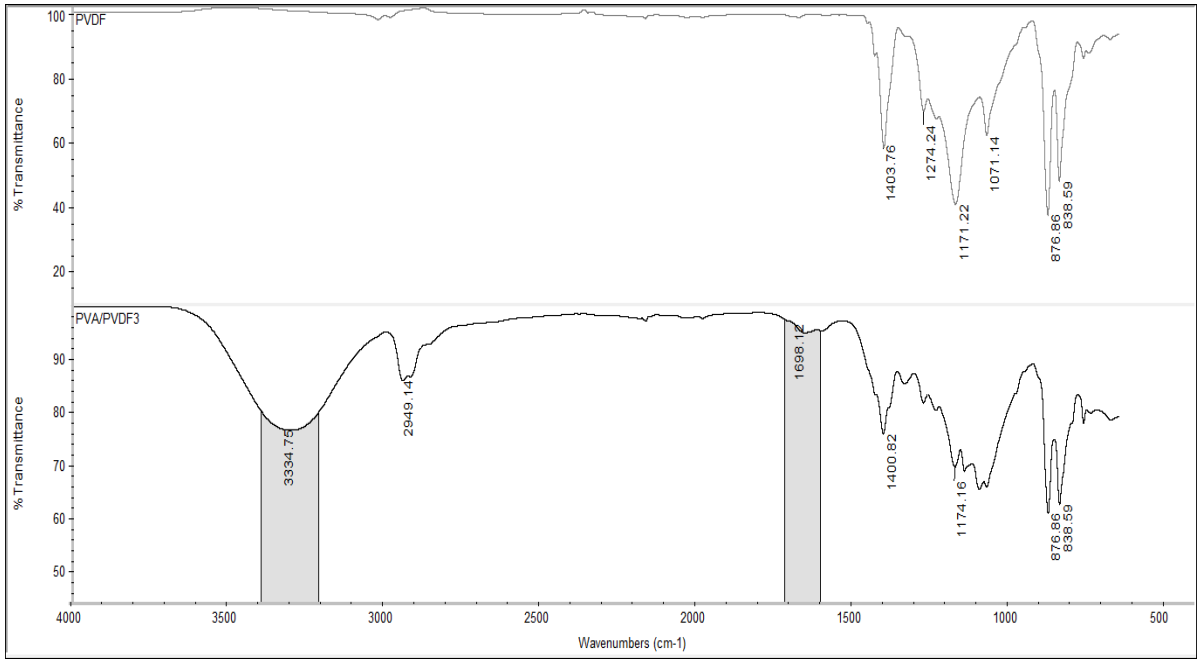

Fig. 4. FTIR spectra of pristine PVDF and PVA/PVDF3 composite membranes.

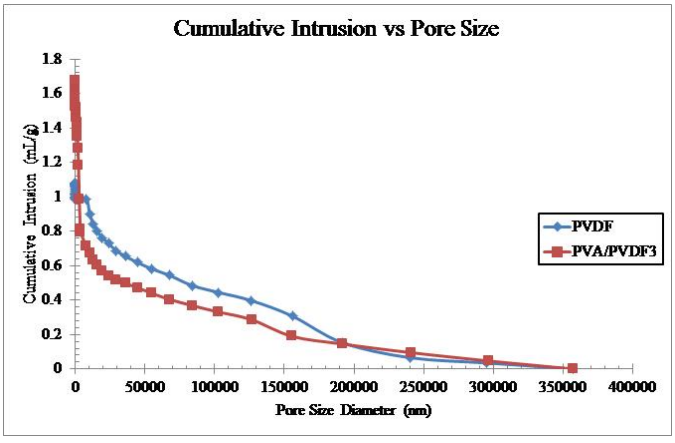

Fig. 5. Cumulative intrusion vs pore size curves of pristine PVDF and PVA/PVDF3 composite membranes.

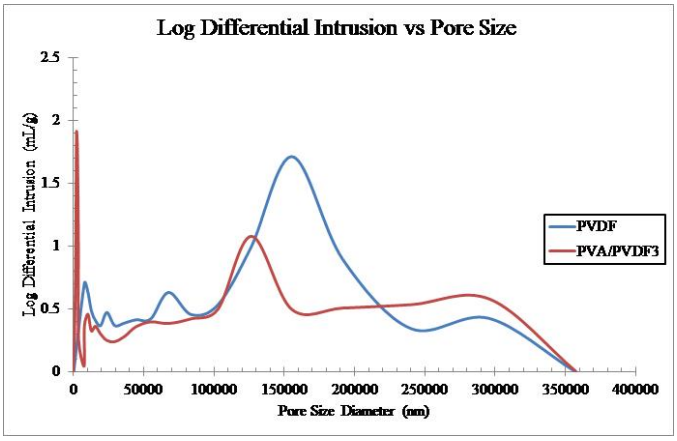

Fig. 6. Log differential intrusion vs pore size curves of pristine PVDF and PVA/PVDF3 composite membranes.

Furthermore, it is worth mentioning that during the cross-linking process of the remelted PVA nanofibers (after water vapour exposure) on PVDF nanofibrous substrate in the cross-linking bathes, the residual uncross-linked fraction of hydroxyl groups of PVA provided the inter and intra molecular hydrogen bonding at the interface of PVA and PVDF layers in the composite membranes. Hence, the H-bonding between these polymers reduced the possibility for partial dissolution of PVA top layer from the substrate which can be attributed to the long-term operation of the resultant composite membranes. In addition to the saline, it is predicted that the FO performance of microorganisms or organics using PVA/PVDF3 composite membranes fabricated in this study will result in a desirable reverse solute flux as an advantage of their larger size. However, the larger sizes of organic compounds compared with inorganics compounds (for example, the use of NaCl in this current work) will cause the slow diffusion across the porous substrate that leads to enhanced ICP.

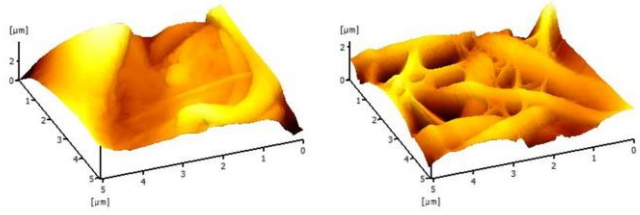

Fig. 7. AFM images of (a) pristine PVDF and (b) PVA/PVDF3 composite membranes.

Table 5
Surface roughness of pristine PVDF and composite membranes.

Membrane	Ra (nm)	Rq/RMS (nm)	Rz/Rmax (nm)
PVDF	89.55	112.2	519.0
PVA/PVDF3	67.21	76.79	263.5

4. Conclusions

This study observed that the PVA thin layer was successfully fabricated and cross-linked on PVDF nanofiber support via HCl-catalysed acetalisation with GA which is proven in terms of morphologies, elemental analysis, increased in hydrophilicity, surface functional groups, porosity and surface roughness. Therefore, this study indicated that surface-coated of electrospun hydrophobic PVDF nanofiber membrane support layer with cross-linked PVA is a useful approach to overcome the drawback of the existing issues in the conventional method of manufacturing TFNC membranes. Based on the FO performance, the next novel modifications and improvements can be further explored to achieve a desirable dual-layered cross-linked PVA on electrospun PVDF nanofibers which can sustain a steady FO performance for long-term operation without compromising the water flux and reverse salt flux. Furthermore, it could be a viable alternative in the preparation of dual-layered composite membranes consist of ENMs as the support layer and cross-linked PVA top coating as the active layer, to be utilised in other membrane technology applications (e.g., seawater desalination using FO membrane), as an addition to the existing applications to resolve the contemporary global water issue.

Acknowledgements

The authors would like to thank the Ministry of Higher Education (MOHE) and Universiti Teknologi Malaysia (UTM) for the financial support from the grant with vote number R.J090301.7846.4J184. Sincerest gratitude is also conveyed to the Research Management Centre (RMC) of Universiti Teknologi Malaysia (UTM) for supporting the research management activities. This research was also supported by the Japan International Cooperation Agency with the award number of R.J130000.7351.4B356.

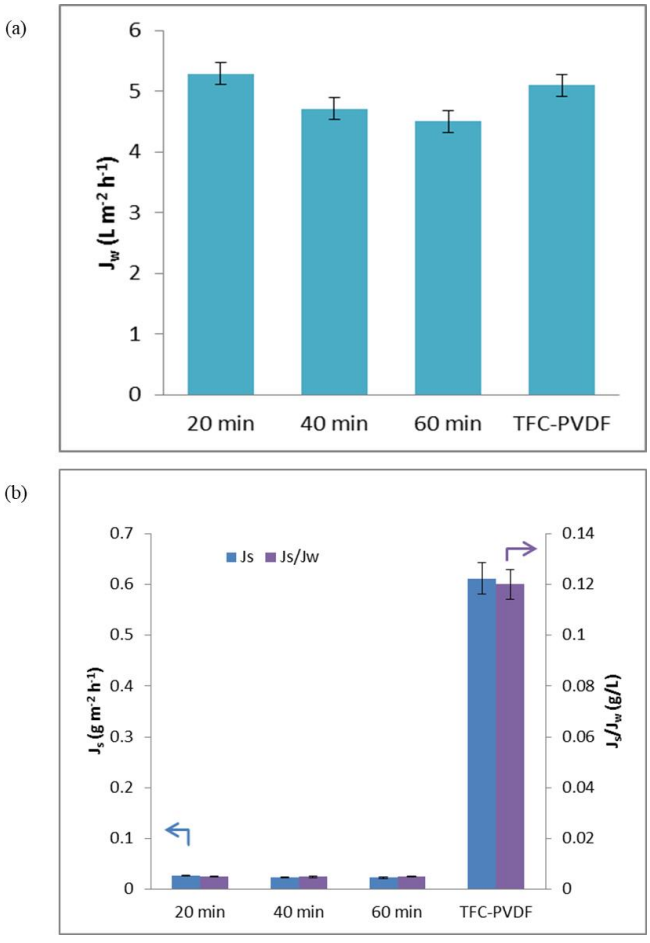

Fig. 8. (a) Water flux and (b) reverse salt flux and specific salt flux of the prepared PVA/PVDF3 composite membranes and control TFC-PVDF membrane.

References

[1] V.G. Gude, N. Nirmalakhandan, S. Deng, Renewable and sustainable approaches for desalination, Renew. Sustain. Energy Rev. 14 (2010) 2641-2654. doi:https://doi.org/10.1016/j.rser.2010.06.008.

[2] Y. Liao, C.-H. Loh, M. Tian, R. Wang, A.G. Fane, Progress in electrospun polymeric nanofibrous membranes for water treatment: Fabrication, modification and applications, Prog. Polym. Sci. 77 (2018) 69-94. doi:https://doi.org/10.1016/j.progpolymsci.2017.10.003.

[3] M. Huang, L. Meng, B. Li, F. Niu, Y. Lv, Q. Deng, J. Li, Fabrication of innovative forward osmosis membranes via multilayered interfacial polymerization on electrospun nanofibers, J. Appl. Polym. Sci. 136 (2019) 47247. doi: https://doi.org/10.1002/app.47247.

[4] J. Shi, H. Kang, N. Li, K. Teng, W. Sun, Z. Xu, X. Qian, Q. Liu, Chitosan sub-layer binding and bridging for nanofiber-based composite forward osmosis membrane, Appl. Surf. Sci. 478 (2019) 38-48. doi:https://doi.org/10.1016/j.apsusc.2019.01.148.

[5] M. Ghanbari, D. Emadzadeh, W.J. Lau, H. Riazi, D. Almasi, A.F. Ismail, Minimizing structural parameter of thin film composite forward osmosis membranes using polysulfone/halloysite nanotubes as membrane substrates, Desalination 377 (2016) 152-162. doi:https://doi.org/10.1016/j.desal.2015.09.019.

[6] X.F. Wang, K. Zhang, Y. Yang, L.L. Wang, Z. Zhou, M.F. Zhu, B.S. Hsiao, B. Chu, Development of hydrophilic barrier layer on nanofibrous substrate as composite membrane via a facile route, J. Membr. Sci. 356 (2010) 110-116. doi:https://doi.org/10.1016/j.memsci.2010.03.039.

[7] L. Shen, X. Yu, C. Cheng, C. Song, X. Wang, M. Zhu, B.S. Hsiao, High filtration performance thin film nanofibrous composite membrane prepared by electrospraying technique and hot-pressing treatment, J. Membr. Sci. 499 (2016) 470-479. doi:https://doi.org/10.1016/j.memsci.2015.11.004.

[8] V. Beachley, X. Wen, Effect of electrospinning parameters on the nanofiber diameter and length, Mater. Sci. Eng. C Mater. 29 (2009) 663-668. doi:https://doi.org/10.1016/j.msec.2008.10.037.

[9] Z.-M. Huang, Y.-Z. Zhang, M. Kotaki, S. Ramakrishna, A review on polymer nanofibers by electrospinning and their applications in nanocomposites, Compos. Sci. Technol. 63 (2003) 2223-2253. doi:https://doi.org/10.1016/S0266-3538(03)00178-7.

[10] S. Nasreen, S. Sundarrajan, S. Nizar, R. Balamurugan, S. Ramakrishna, Advancement in electrospun nanofibrous membranes modification and their application in water treatment, Membranes 3 (2013) 266-284. doi: https://doi.org/10.3390/membranes3040266.

[11] Z. Tang, J. Wei, L. Yung, B. Ji, H. Ma, C. Qiu, K. Yoon, F. Wan, D. Fang, B.S. Hsiao, B. Chu, UV-cured poly(vinyl alcohol) ultrafiltration nanofibrous membrane based on electrospun nanofiber scaffolds, J. Membr. Sci. 328 (2009) 1-5. doi:https://doi.org/10.1016/j.memsci.2008.11.054.

[12] X. Wang, D. Fang, K. Yoon, B. Hsiao, B. Chu, High performance ultrafiltration composite membranes based on poly (vinyl alcohol) hydrogel coating on crosslinked nanofibrous poly (vinyl alcohol) scaffold, J. Membr. Sci. 278 (2006) 261-268. doi:https://doi.org/10.1016/j.memsci.2005.11.009.

[13] M.J. Park, R.R. Gonzales, A. Abdel-Wahab, S. Phuntsho, H.K. Shon, Hydrophilic polyvinyl alcohol coating on hydrophobic electrospun nanofiber membrane for high performance thin film composite forward osmosis membrane, Desalination 426 (2018) 50-59. doi:https://doi.org/10.1016/j.desal.2017.10.042.

[14] S.S. Ray, S.-S. Chen, N.C. Nguyen, H.-T. Hsu, H.T. Nguyen, C.-T. Chang, Poly(vinyl alcohol) incorporated with surfactant based electrospun nanofibrous layer onto polypropylene mat for improved desalination by using membrane distillation, Desalination 414 (2017) 18-27. doi:https://doi.org/10.1016/j.desal.2017.03.032.

[15] M. Obaid, Z.K. Ghouri, O.A. Fadali, K.A. Khalil, A.A. Almajid, N.A.M. Barakat, Amorphous SiO_2 NP-incorporated poly(vinylidene fluoride) electrospun nanofiber membrane for high flux forward osmosis desalination, ACS Appl. Mater. Interfaces 8 (2016) 4561-4574. doi:https://doi.org/10.1021/acsami.5b09945.

[16] M. Shibuya, M.J. Park, S. Lim, S. Phuntsho, H. Matsuyama, H.K. Shon, Novel CA/PVDF nanofiber supports strategically designed via coaxial electrospinning for high performance thin-film composite forward osmosis membranes for desalination, Desalination 445 (2018) 63-74. doi:https://doi.org/10.1016/j.desal.2018.07.025.

[17] L. Huang, J.T. Arena, J.R. McCutcheon, Surface modified PVDF nanofiber supported thin film composite membranes for forward osmosis, J. Membr. Sci. 499 (2016) 352-360. doi:https://doi.org/10.1016/j.memsci.2015.10.030.

[18] H. You, Y. Yang, X. Li, K. Zhang, X. Wang, M. Zhu, B.S. Hsiao, Low pressure high flux thin film nanofibrous composite membranes prepared by electrospraying technique combined with solution treatment, J. Membr. Sci. 394-395 (2012) 241-247. doi:https://doi.org/10.1016/j.memsci.2011.12.047.

[19] J.A. Prince, G. Singh, D. Rana, T. Matsuura, V. Anbharasi, T.S. Shanmugasundaram, Preparation and characterisation of highly hydrophobic poly(vinylidene fluoride) – clay nanocomposite nanofiber membranes (PVDF–clay NNMs) for desalination using direct contact membrane distillation, J. Membr. Sci. 397-398 (2012) 80-86. doi:https://doi.org/10.1016/j.memsci.2012.01.012.

[20] R. Moradi, J. Karimi-Sabet, M. Shariaty-Niassar, M. Koochaki, Preparation and characterisation of polyvinylidene fluoride/graphene superhydrophobic fibrous films, Polymers 7 (2015) 1444-1463. doi: https://doi.org/10.3390/polym7081444.

[21] C. Wei, F. Dai, L. Lin, Z. An, Y. He, X. Chen, L. Chen, Y. Zhao, Simplified and robust adhesive-free superhydrophobic SiO_2-decorated PVDF membranes for efficient oil/water separation, J. Membr. Sci. 555 (2018) 220-228. doi:https://doi.org/10.1016/j.memsci.2018.03.058.

[22] G.M. Nisola, L.A. Limjuco, E.L. Vivas, C.P. Lawagon, M.J. Park, H.K. Shon, N. Mittal, I.W. Nah, H. Kim, W.-J. Chung, Macroporous flexible polyvinyl alcohol lithium adsorbent foam composite prepared via surfactant blending and cryo-desiccation, Chem. Eng. J. 280 (2015) 536-548. doi:https://doi.org/10.1016/j.cej.2015.05.107.

[23] K.C.S. Figueiredo, T.L.M. Alves, C.P. Borges, Poly(vinyl alcohol) films crosslinked by glutaraldehyde under mild conditions, J. Appl. Polym. Sci. 111 (2009) 3074-3080. doi:https://doi.org/10.1002/app.29263.

[24] A.L. Ahmad, N.M. Yusuf, B.S. Ooi, Preparation and modification of poly (vinyl) alcohol membrane: Effect of crosslinking time towards its morphology, Desalination 287 (2012) 35-40. doi:https://doi.org/10.1016/j.desal.2011.12.003.

[25] M. Huang, Y. Chen, C.-H. Huang, P. Sun, J. Crittenden, Rejection and adsorption of trace pharmaceuticals by coating a forward osmosis membrane with TiO_2, Chem. Eng. J. 279 (2015) 904-911. doi:https://doi.org/10.1016/j.cej.2015.05.078.